Purification and Characterization of Two Cysteine Peptidases of the Mediterranean Fruit Fly *Ceratitis capitata* During Metamorphosis

Alejandro Rabossi,[1] Veronika Stoka,[2] Vida Puizdar,[2] Vito Turk,[2] and Luis A. Quesada-Allué[1]*

In holometabolous insects, there is a complete body remodeling from larva to adult. We determined in *Ceratitis capitata* that the transition from pre-pupa to pupa, 40 to 48 h after puparium formation (h APF), is a key moment of metamorphosis; when salivary glands, intestine, fat body, and muscles are in different stages of cell death. At 44–46 h APF, muscles from segments 1–3 (thoracic region) appeared fully disintegrated, whereas posterior muscles just started death processes. To understand some of the biochemical events eventually involved in histolytic processes during early metamorphosis, two cysteine peptidases coined "Metamorphosis Associated Cysteine Peptidase" (MACP-I and MACP-II) were purified to homogeneity from 40–46-h APF insects. Both enzymes were inhibited by Ep-475, a specific inhibitor of papain-like cysteine-peptidases. MACP-I is a single chain protein with an apparent molecular mass of 80 kDa and includes several isoforms with pI values of pH 6.25–6.35, 6.7, and 7.2. The enzyme has an optimum pH of 5.0 and its pH stability ranges from pH 4.0 to 6.0. The molecular weight and N-terminal sequence suggest that MACP-I might be a novel enzyme. MACP-II is an acidic single chain protein with a pI of pH 5.85 and an apparent molecular mass of 30 kDa. The enzyme is labile with a maximum stability in the pH range of 4.0 to 6.0 and an optimum pH among 5.0 to 6.0. MAPCP-II characteristics suggest it is a cathepsin B-like enzyme. Arch. Insect Biochem. Physiol.

KEYWORDS: Diptera; larval tissue histolysis; papain-like enzyme; proteinases; cathepsins

INTRODUCTION

Metamorphosis in holometabolous insects is the transition from the immature to the adult forms. During this process, most of the larval tissues are histolyzed and adult ones are generated by expansion and differentiation of imaginal discs and histoblasts. The whole process is triggered by the molting hormone 20-OH-ecdysone (Riddiford et al., 2003), which leads to the transcription of metamorphosis-specific genes. The intermediate metamorphic stage is called pupal stage, a period of huge transformations. It is generally accepted that pupation begins with the onset of larval-pupa apolysis. We previously determined in the Mediterranean fruitfly (medfly) *C. capitata* that apolysis occurs 20:30 h after puparium formation (APF) (Rabossi et al., 1991). After apolysis, the secretion

[1]Department of Biological Chemistry, FCEyN, Universidad de Buenos Aires, IIBBA-CONICET and Fundación Instituto Leloir, Buenos Aires, Argentina

[2]Department of Biochemistry, Molecular and Structural Biology, J. Stefan Institute, Ljubljana, Slovenia

Alejandro Rabossi and Veronkia Stoka contributed equally to this work.

Contract grant sponsor: University of Buenos Aires; Contract grant sponsor: CONICET; Contract grant sponsor: ANPCyT of Argentina; Contract grant sponsor: Ministry of Higher Education, Science and Technology of the Republic of Slovenia; Contract grant number: P1-0140.

Abbreviations used: APF = after puparium formation; MACP-I = metamorphosis-associated cystein peptidase I; MACP-II = metamorphosis-associated cystein peptidase II; Z-FR-AMC = benzyloxycarbonyl-Phe-Arg-7-amido-4-methylcoumarin; Z-FVR-AMC = benzyloxycarbonyl-Phe-Val-Arg-7-amido-4-methylcoumarin.

*Correspondence to: Luis A. Quesada-Alluzé, Instituto de Investigaciones Bioquimicas-CONICET, Patricias Argentinas 435, (1405) Buenos Aires, Argentina.
E-mail: lualque@iib.uba.ar

Received 9 July 2007; Accepted 18 October 2007

DOI: 10.1002/arch.20231
Published online in Wiley InterScience (www.interscience.wiley.com)

of pupal cuticle occurs and the insect remains with the head invaginated and the thoracic appendages undifferentiated ("cryptocephalic" pupa). The transformation from "cryptocephalic" to "phanerocephalic" (everted head) pupa consists of head evagination and the expansion of the thoracic appendages (Fig. 1). In *C. capitata*, this transition occurs in a period of 6 h (40 to 46 h APF). Some authors accepted that this is the end of the pupation process (Zdarek, 1985), but for *C. capitata*, we proposed that pupation ends at 72 h APF, when both the definitive shape of the head and final body proportions are attained. At this moment, full deposition of cuticle proteins is also complete (Rabossi et al., 1991, 1992).

In higher Diptera, at a given time of pupation, most of the larval tissues are at different stages of histolysis process (Fig. 1). Relatively few studies exist on the identity and role of peptidases during the peculiar cell death process giving rise to complete histolysis of larval tissues. In the Medfly, we described a temporal correlation between metamorphosis progress and the overall lysosomal proteolytic activity, catalyzed by aspartic and cystein proteinases (Rabossi and Quesada-Allué, 2000). This process involves the sequential dissociation of fat body adipocytes, followed by nuclear and cellular lysis (Rabossi et al., 2004). The aspartic proteinase appears at the onset of pupation, simultaneously with the cystein peptidases shown here. Recently, Gui et al. (2006) studied a similar Cathepsin D in the silkworm *Bombyx mori*.

In insects, cysteine peptidases were found to participate mainly in four major events, (1) the hydrolysis of yolk proteins during embryogenesis (Zhao et al., 2002, 2005), (2) proteolysis of dietary proteins in the digestive tract of larvae (Brown et al., 2004), (3) intracellular protein turnover in the lysosomes (Scott et al., 2004) and, (4) larval tissue histolysis during metamorphosis (Kawamura et al., 1984), in particular fat body dissociation during metamorphosis (Kurata et al. 1990; Xu and Kawasaki, 2001). Cysteine peptidases were also involved in *B. mori* silk gland histolysis (Shiba et al., 2001) and in the decomposition of the adult fat body during aging and oogenesis (Yang et al., 2006).

We previously determined that the fat body disintegration progresses in an anterior–posterior way (Rabossi et al., 2004). We are currently assuming that larval muscle histolysis must progress in the same direction, taking into account that the evagination of the head and inflation of the appendages is attained by abdominal muscles (Zdarek and Friedman, 1986). Here we report the isolation and partial biochemical characterization of the two main cystein peptidases registered during early metamorphosis of the Mediterranean fruit fly (medfly) *C. capitata*, at the onset of the pupal stage.

MATERIALS AND METHODS

Chemicals

All the reagents were of analytical grade. The substrates benzyloxycarbonyl-Phe-Arg-7-amido-4-methylcoumarin (Z-FR-AMC) and benzyloxycarbonyl-Phe-Val-Arg-7-amido-4-methylcoumarin (Z-FVR-AMC) were from Bachem (Bubendorf, Switzerland). The cysteine peptidase inhibitor L-3-carboxy-2,3-trans-epoxypropionyl-leucylamido-(3-methyl)butane (Ep-475) was from the Peptide Research Institute (Saitama, Japan). The gels Sephacryl S-200, Thiol-Sepharose 4B, the chromatographic columns Mono S (HR 5/5) and Superose 12, as well as the precasted gels for the PhastSystem apparatus and the Broad pI Kit (pH 3.5 to 9.3) were from Pharmacia (Uppsala, Sweden). The protein assay kit was from Bio-Rad (Hercules, CA). Other reagents were from Sigma-Aldrich (St. Louis, MO) unless otherwise stated. Stock solutions of the substrates and the inhibitor were prepared in dimethyl sulphoxide.

Insects

Wild type *C. capitata* ("INTA Arg 17") were reared on a carrot-based diet as described by Quesada-Allué et al. (1994). Our results refer to a standard life cycle at 23°C and 50–70% relative humidity with a 16L:8D photoperiod (Rabossi et al., 1992). Age within the puparium is expressed in hours after (APF) or before (BPF) puparium formation, starting at the definitive immobilization

of the third instar larva, previously defined as "zero time" (Rabossi et al., 1991).

Purification of Medfly Cysteine Peptidases

C. capitata (40–46 h APF) pupae were subjected to homogenization and acid activation at pH 4.2. The precipitated proteins from 30 to 70% ammonium sulfate salting out were solubilized and dialyzed in 100 mM sodium acetate buffer, pH 5.5, containing 1 mM EDTA and 300 mM NaCl (buffer 1). The material was applied to a Sephacryl S-200 gel filtration column equilibrated at 33.3 ml/h flow rate and 5 ml fractions were collected. After chromatography, the active fractions labeled as peaks I and II were pooled, concentrated, and dialyzed against 100 mM sodium phosphate buffer, pH 6.0, containing 1 mM EDTA and 300 mM NaCl (buffer 2). Each active peak was further purified on Thiol-Sepharose 4B covalent chromatography (Brocklehurst et al., 1973). Briefly, the gel matrix and the sample were coupled by mixing at 37°C for 2 h. Then, the column was filled with the mixture, and after all of the unbound material was washed with buffer 2, the bound proteins were eluted with 20 mM cysteine dissolved in the same buffer. The bound active fractions were pooled, concentrated, and dialyzed against 20 mM sodium acetate buffer, pH 5.0, containing 1 mM EDTA (buffer 3) and subjected to cation exchange chromatography on a Mono S (HR 5/5) column of Pharmacia Fast Protein Liquid Chromatography (FPLC) system. After elution of all unbound proteins with buffer 3, a linear NaCl gradient in buffer 3 was applied (0–0.7 M, 35 ml for peak I and 0–0.3 M, 45 ml for peak II, respectively). The fractions were eluted at 1 ml/min flow rate. The peaks of activity were named "Metamorphosis Associated Cysteine Peptidase I" (MACP-I) and "Metamorphosis Associated Cysteine Peptidase II" (MACP-II), respectively. SDS-gel electrophoresis of MACP-II confirmed the purity to homogeneity of this peptidase. The pooled active fractions corresponding to MACP-I were concentrated to 0.5 ml and further purified by gel filtration on a Superose 12 column of Pharmacia FPLC system. The column was equilibrated with 20 mM sodium acetate buffer, pH 5.0, containing 1 mM EDTA and 300 mM NaCl, at a flow rate of 0.5 ml/min. The active fractions were pooled and the material submitted to SDS-gel electrophoresis to assess the degree of purity. The protein concentration was determined using Bio-Rad Protein Assay, based on Bradford's method. During the enzyme purification, protein was routinely monitored by measurement of absorbance at 280 nm on a Perkin Elmer UV/VIS spectrometer Lambda 11.

Enzymatic Assays

Cysteine peptidase activity was monitored by the hydrolysis of fluorogenic substrates Z-FR-AMC or Z-FVR-AMC (Turk et al., 1994). Briefly, the reaction was carried out in 150 mM sodium acetate buffer, pH 5.5, containing 2 mM EDTA. Prior to the reaction, the stock solution of the substrate were dissolved in the reaction buffer (250 μM final concentration). Ten microliters of the sample was added to 490 μl of 2× reaction buffer plus 250 μl of dithiothreitol (2 mM final concentration) and pre-incubated for 5 min at 37°C. Then, the mixture was incubated for 10 min with 250 μl of substrate (20 μM) and the reaction was stopped by addition of 2 ml of 1 mM iodoacetic acid. The fluorescence of the released aminomethylcoumarin was measured on a Perkin Elmer Luminescence Spectrometer LS50B at excitation and emission wavelengths of 370 and 460 nm, respectively. One unit of activity was defined as the amount of enzyme that hydrolyses 1 μM substrate/min. To test the cysteinase identity, the cysteine peptidase inhibitor Ep-475 was pre-incubated with 200 μl of enzymatic extract at 4°C, after which the reaction was triggered by addition of the fluorogenic substrate and the mixture incubated at 37°C as described above.

Optimum pH and pH Stability

The reaction buffers were 100 mM phosphate-citrate buffer pH 2.0 to 7.0 and 100 mM Tris-HCl buffer, pH 8.0. Optimum pH was determined by incubation of the enzyme at 37°C; 5 min without substrate and then 10 min, using Z-FVR-AMC for

MACP-I and Z-FR-AMC for MACP-II as substrates. The pH stability was determined by pre-incubation of the enzyme at 37°C with the above buffers of different pH in the absence of substrates (120 min for MACP-I and 15 min for MACP-II). The residual enzymatic activity was then measured as above, during 10 min.

SDS-PAGE and Isoelectric Focusing

Sodium dodecyl sulfate polyacrylamide gel electrophoresis (SDS-PAGE) was carried out on a PhastSystem apparatus on a Phast-Gel Gradient 8-25 for 30 min at 250 V, following the manufacturer's instructions (Pharmacia). Samples (3 µl) were diluted with 0.02% bromophenol blue in Tris buffer pH 8.0 containing 2 mM EDTA, 5% SDS at 1:1 ratio (v/v). Samples were reduced by adding 10% 2-mercaptoethanol and boiled for 5 min. After electrophoresis, the gel was stained with a 0.02% Phast-Gel blue R in 0.1% $CuSO_4$ containing 30% methanol and 10% acetic acid. The gel was calibrated using the following molecular mass markers: phosphorylase B (94 kDa), bovine serum albumin (67 kDa), ovoalbumin (43 kDa), bovine erythrocyte carbonic anhydrase (30 kDa), soybean trypsin inhibitor (20.1 kDa), and α-lactalbumin (14.4 kDa). The isoelectric point (pI) of the cysteine peptidases was determined by analytical isoelectric focusing (IEF) carried out on a PhastSystem apparatus following the manufacturer's instructions (Pharmacia). The pH gradient 3 to 9 was performed on a Phast-Gel IEF gel 3-9 at 2,000 V. Then, 3 µl of samples (~0.5 mg/ml) and the protein standards were applied on the above gel to be focused for 30 min from 200 to 2,000 V. After electrophoresis, the proteins were fixed with 20% trichloroacetic acid and stained with 0.02 % Coomassie brilliant blue R-250. For pI determination, the following proteins standards were used: amyloglucosidase (3.50), soybean trypsin inhibitor (4.55), β-lactoglobulin A (5.20), bovine carbonic anhydrase B (5.85), human carbonic anhydrase B (6.55), horse myoglobin-acidic band (6.85), horse myoglobin-basic band (7.35), lentil lectin-acidic band (8.15), lentil lectin-middle band (8.45), lentil lectin-basic band (8.65), and trypsinogen (9.30).

Histological Studies

The pupae were fixed in Bouin fixative and after not less than 24 h fixation at room temperature, transvere sections between the 4th and the 5th segments were prepared and fixed again in Bouin for 24 h. After two washes with distilled water, the material is dehydrated with the classical alcohol series, embedded in paraffin and sectioned in a glass-blade microtome. Sections (10 µm) were stained with hematoxylin-eosin, mounted and analyzed using a camera-attached microscope (Zeiss, model Axioplan MC 80, Oberkochen, Germany).

N-Terminal Amino Acid Sequence

Prior to N-terminal sequencing, the samples were desalted on a Chrompack chrom Spher C8 column on a LDC Milton Roy HPLC Chrompack CromSpher C8 system (Oregon City, OR). The column was equilibrated at 1 ml/min flow rate and extensively washed with 0.1% trifluoroacetic acid and the proteins were eluted with a linear gradient of 0–70% acetonitrile containing 0.1% trifluoroacetic acid. The protein concentration was detemined by the UV monitoring at 215 nm and continuously recorded. The samples were dried on a Savant Speed-Vac apparatus and resuspended in 20% acetontrile. The N-terminus of MACP-I and MACP-II were determined automatically according Edman's degradation on an Applied Biosystems liquid phase sequenator 475A. Phenylthiohydantoin derivatives were identified on line with the Applied Biosystems HPLC 120A. The reduced and alkylated protein were hydrolyzed with 6 M HCl at 110°C for 24 and 72 h. Amino acid compositions were determined using a Beckman 118CL analyzer, by post-column fluorescence detection after reaction with o-phthaldialdehyde.

RESULTS

Early Metamorphosis Events

We followed the progress of *Ceratitis capitata* tissue disintegration during metamorphosis in the standardized life cycle (see Materials and Methods), which includes the beginning and span of the histolytic process for different tissues of *C. capitata*, from

the end of the third larval stage ("zero time") until the end of the pharate stages (314 h APF) (Fig. 1).

During the last hours of the third larval stage, the salivary glands and digestive tract showed the first signs of histolysis (Fig. 1). Then, starting around the time of larval-pupal apolysis (20 h 30 min APF), the anterior fat body and muscles corresponding to larval segments 1 to 4 progressively disintegrated, ending at 72 and 44–46 h APF, respectively (Fig. 1). The posterior fat body and muscles (corresponding to the larval abdominal region) started to disintegrate later, at 40 h APF, just at the beginning of the pupal stage, i.e., when the first pupal cuticle proteins are deposited (Boccaccio and Quesada Allué, 1989). During this transition from pre-pupa to pupa stages, called the cryptocephallic stage, the head is invaginated and starts to emerge at 44–46 h APF (Fig 1, bottom). The fully evaginated head and definitive body proportion are attained 72 h APF (Fig 1, bottom); when the anterior fat body as well as most of the salivary glands are fully disintegrated.

At 46 h APF, a pupal cuticle is already formed (Fig. 2A,B). Figure 2 shows the degree of muscle (Fig. 2C,D) and fat body (Fig. 2E,F) disintegration at the time of head evagination (44–46 h APF). The muscle cells corresponding to thoracic segments 1–3 are completely disintegrated (Fig. 2A,C). However, at the same time, abdominal muscles seem to remain normal (Fig. 2B,D). This was expected, since functional muscles are required to start the peristaltic contractions leading to complete evagination of the head and appendices (48 h APF). At 46 h APF, the nuclear membrane of the anterior fat body cells started to dissociate whereas the plasma membrane was less defined and difficult to recognize (Fig. 2E). A significant amount of vesicles close to the plasma membrane was observed (Fig. 2E). In agreement with the muscle images in the posterior region (Fig. 2D), the nuclei and plasma membrane of the posterior fat body remained normal (Fig. 2F).

Cystein Proteinase Activity

At the start of the pupal stage (40 h APF), which is the time of maximum cystein peptidase activity, we found that total cysteine peptidase activity accounts for from 35 to 40% of the total proteolytic activity against hemoglobin. The overall cysteine peptidase activity 8 h before puparium formation (end of Larval III stage) was 0.0121 E.U./mg and then increased during the pre-pupal stage to 0.0287 Hb.E.U./mg protein at the time of apolysis (20:30 h APF, Fig. 1). The maximum activity attained was 40 h APF (0.0468 Hb.E.U./mg protein), which then decayed to 0.0071 Hb.E.U./mg protein at 72 h APF (anterior fat body full lysis). Thus the increase in cysteine peptidase activity correlated well with both the start of the pupal stage and with the observed anterior muscles and fat body disintegration.

Isolation of MACP-I and MACP-II

Two main early metamorphosis cysteine peptidases, "Metamorphosis Associated Cysteine Peptidase-I" (MACP-I) and "Metamorphosis Associated Cysteine Peptidase-II" (MACP-II), were purified from *C. capitata* pupae 40–46 h APF that were disrupted to release a rich proteolytic extract. This step was followed by an acid activation at pH 4.2 and a 30 to 70% ammonium sulfate salting out. The resulting material was applied to a Sephacryl S-200 gel filtration column (Fig. 3A). The enzymatic activity was monitored with the fluorogenic substrate benzyloxycarbonyl-Phe-Arg-7-amido-4-methylcoumarin (Z-FR-AMC) and the activity profile showed two main peaks, namely peak I (fractions 50–62) and peak II (fractions 80–90) (Fig. 3A). These activities belonging to peak I and peak II were abolished by the general papain-like cysteine peptidases inhibitor, Ep-475 (97 and 99% inhibition, respectively). The pooled fractions belonging to peaks I and II were separately purified by covalent chromatography on Thiol-Sepharose 4B columns (not shown) and the bound material further analyzed by gel electrophoresis. The degree of purification attained is shown by SDS-PAGE profiles of the adsorbed proteins (insets to Figure 3B and C, respectively). The bound material resulting from each covalent chromatography that exhibit cysteine peptidase activity was subjected to cation-exchange chromatography on Mono S columns, as shown

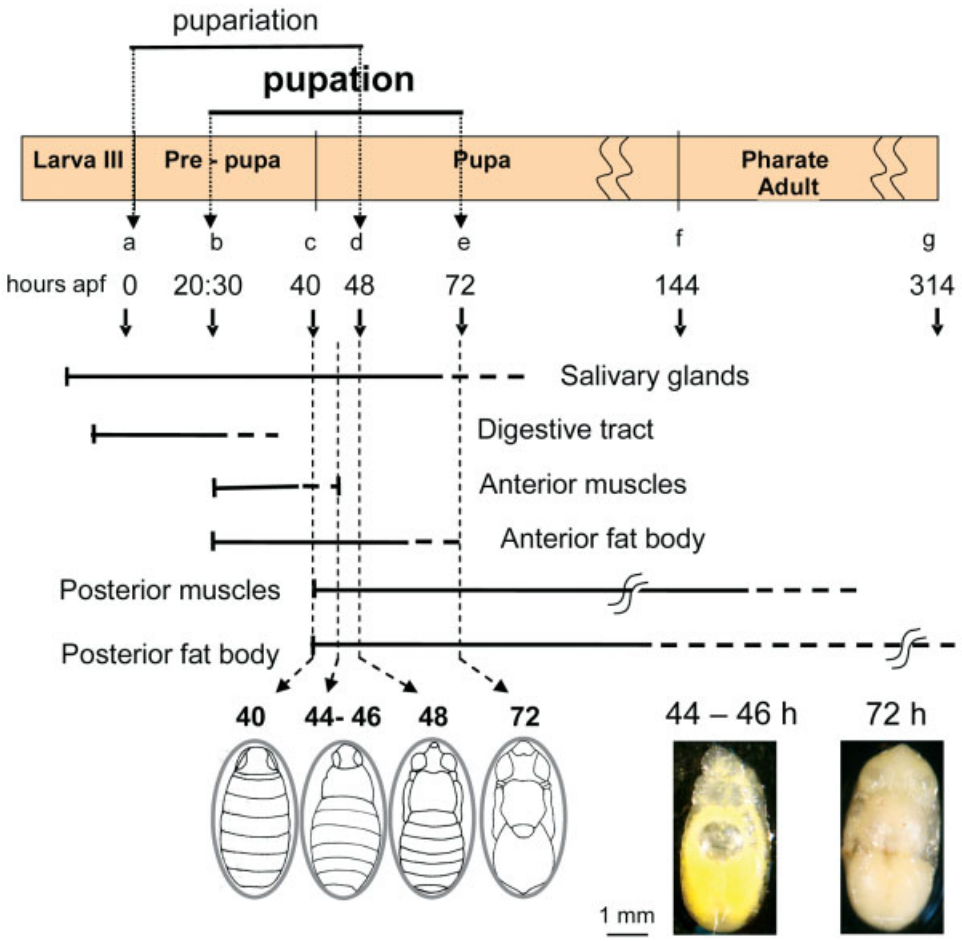

Figure 1.

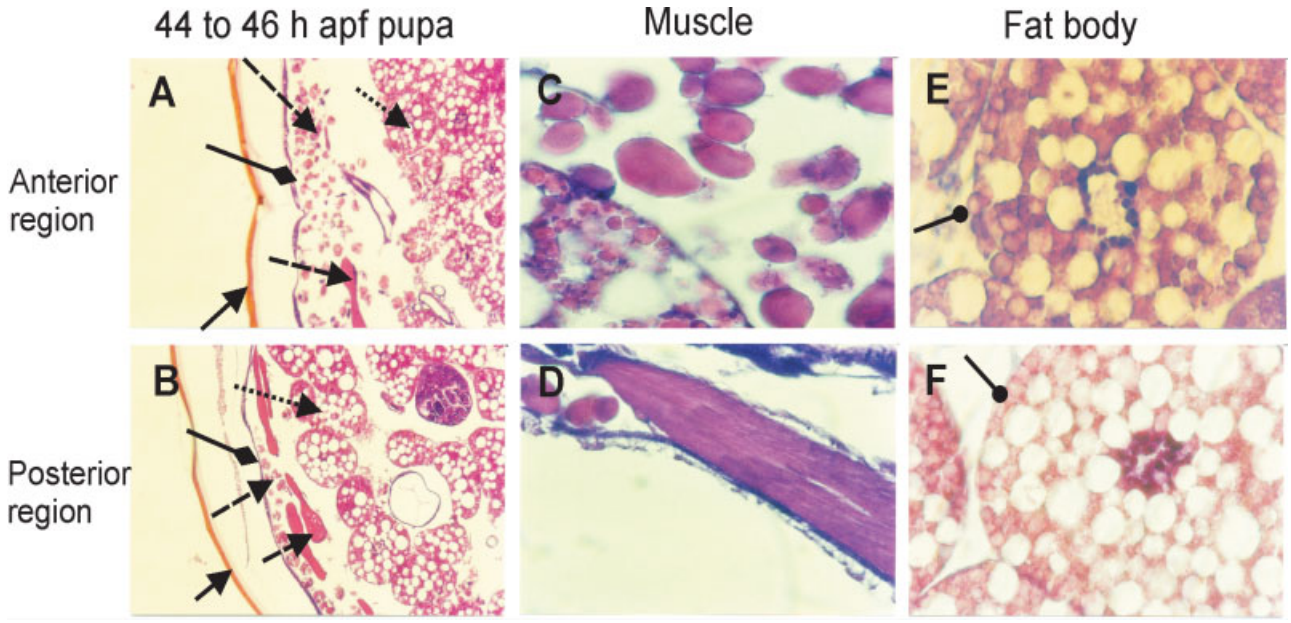

Figure 2.

in Figure 3B and C. Both columns showed two peaks of activity and for practical considerations the material eluting at a high salt concentration was used for further characterization. Thus, the enzymatic activity associated to peak I that eluted at 0.3 M NaCl (Fig. 3B) was denoted MACP-I. The last purification step for this peptidase was carried out by gel filtration on Superose 12 column (not shown).

The enzyme activity associated with peak II that eluted at 0.6 M NaCl in Mono S column (Fig. 3C) was denoted MACP-II. This material required no further purification.

Biochemical Characterization of MACP-I and MACP-II

The material corresponding to MACP-I and MACP-II purified to homogeneity showed activities that were enhanced in the presence of a reducing agent such as cysteine or dithiothreitol and inhibited by the cysteine peptidase inhibitor Ep-475, thus confirming that the enzymes are cysteine peptidases (not shown).

The purified MACP-I is a single chain protein with an estimated molecular mass of 80 kDa, as seen on SDS-PAGE under non-reducing (Fig. 4A, lane 1) and reducing (Fig. 4A, lane 2) conditions, respectively. Upon IEF, the enzyme exhibited a major isoform with a pI between 6.25–6.35 and two minor ones with pIs of 6.7 and 7.2, respectively (Fig. 4B, lane 1). During the isolation procedure, the enzyme activity was routinely followed using the Z-FR-AMC substrate. However, the rate of substrate hydrolysis was considerably higher with Z-FVR-AMC. The latter substrate was further used to determine the optimum pH (5.0) and pH stability (4.0 to 6.0) of this enzyme, as shown in Figure 5A. The N-terminus of MACP-I, VNIESDTADQ, showed a very low sequence homology compared to other N-terminal sequences from insects, invertebrates, or higher eukaryotes.

The purified MACP-II is a single chain acidic protein with an apparent molecular mass of 30 kDa (Fig. 4A, lanes 4–5) and pI close to pH 5.85 (Fig. 4B, lane 3). MACP-II has a broad optimum pH from 4. to 6.0, as monitored using Z-FR-AMC substrate (Fig. 5B). No activity was registered at pH 7.0 probably due to a rapid inactivation at a pH higher than 6.0 (pH stability had to be assayed after 15 min incubation since longer times rapidly abolished the activity) (Fig. 5B). The N-terminal sequence of MACP-II, LPEQFE-P-QF, suggested that it is a cathepsin-like enzyme and showed a consensus proline residue in the second position, which is shared by cysteine peptidases, clan CA, which include papain, cathepsins, and other papain-like enzymes (Rawlings and Barrett, 2004).

DISCUSSION

This is the first report of two cysteine peptidases (MACPs) of *C. capitata* isolated during metamorphosis and purified to homogeneity (Fig. 4A). MACP-II is a papain-like enzyme, whereas MACP-I apparently represents a novel cysteine peptidase. Using inhibition assays with E-64, the total cysteine peptidase activity accounts for from 35 to 40% of the total proteolytic activity against hemoglobin at 40 h APF, which is the time of maximum cystein peptidase activity. The remaining 60% of proteolytic activity corresponds to the previously described aspartic proteinase (Rabossi et al., 2004).

Fig. 1. Progression of larval tissue histolysis and main developmental events during *C. capitata* metamorphosis. The top bar represents the standardized life cycle. Age within the puparium is expressed in hours after puparium formation (APF) starting at "zero time." The horizontal lines indicate the span of each tissue histolysis; dashed ends indicate the degree of uncertainety. Bottom schemes (left) represent the transition from cryptocephalic to definitive body size pupae, drawn from microscope observations as shown (bottom right). (a) "Zero time" of metamorphosis; (b) larval-pupal apolysis (20:30 h APF); (c) cryptocephalic pupa; beginning of the pupal stage (40 h APF); (d) head eversion (48 h APF); (e) definitive body proportions (72 h APF); (f) beginning of the pharate adult stage (144 h APF); (g) imago ecdysis (314 h APF).

Fig. 2. Fat body and muscle disintegration. A,C, E, and B, D, F: anterior and posterior regions of the body, respectively. **A,B:** Trasversal cut (400×). Solid arrows = the puparium; solid diamonds = pupal cuticle; dashed arrows = muscles; dotted arrows = fat body. **C,D:** Longitudinal muscles (1,000×). **E,F:** Fat body cells (1,000×); oval arrows = plasma membrane.

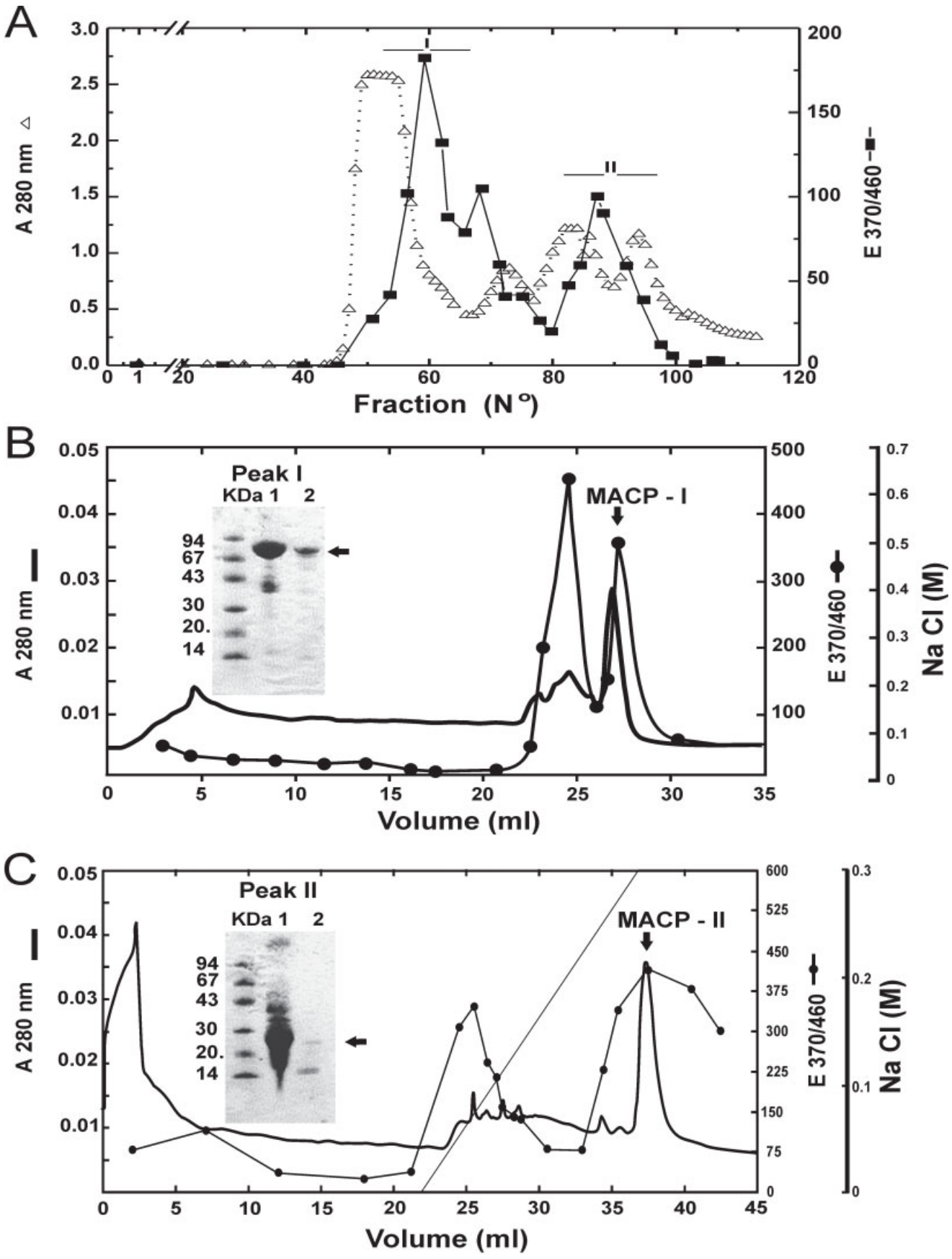
A
A 280 nm
E 370/460
Fraction (N°)
I
II
B
Peak I
KDa 1 2
94
67
43
30
20.
14
MACP - I
A 280 nm
E 370/460
Na Cl (M)
Volume (ml)
C
Peak II
KDa 1 2
94
67
43
30
20.
14
MACP - II
A 280 nm
E 370/460
Na Cl (M)
Volume (ml)

Figure 3.

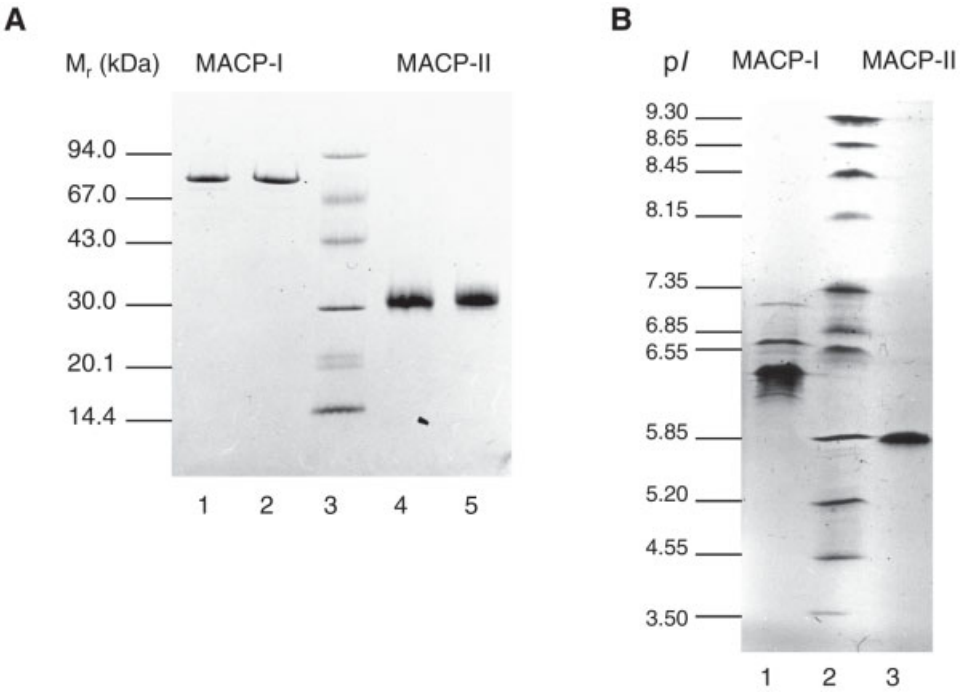

Fig. 4. SDS-PAGE and isoelectric focusing of MACP–I and MACP–II. **A:** SDS-PAGE was carried out under non-reducing (lanes 1 and 4) and reducing (lanes 2 and 5) conditions; lane 3: protein standards. **B:** Isoelectric focusing; lane 2: protein standards.

The two peptidases, MACP-I and MACP-II, were purified from medflies at 40–46 h APF, the transition period from pre-pupa to the pupal stage (Boccaccio and Quesada-Allué, 1989). At 40 h APF, the cryptocephalic pupa, has not yet everted its head and appendages (Rabossi et al., 1992), and the thoracic muscles (not shown) and digestive tract are at the terminal lysis phase of the histolytic process (Fig. 1). Meanwhile, the salivary glands and the anterior fat body (Fig. 1) are in an advanced stage of tissue disruption. In contrast, at 40 h APF, the abdominal muscles and posterior fat body are just starting histolysis. The time of head eversion (44–48 h APF) is coincident with the end of anterior muscles disintegration, intermediate fat body disintegration, and cystein proteinases activity. Thus, a good correlation was established among these histolytic events.

The N-terminal decamer from MACP-I (VNIESDTADQ) is rich in amino acids that scored poorly in most sequence comparisons. Moreover, a BLAST search (Altschul et al., 1990) identified proteins with sequence homologies below 40%, and in spite of the conserved Aspartic in the 6th position (present in papains), no cysteine peptidases were found. The sequence showed very low homology when compared to any other protein from eukaryotes. These preliminary data suggest it might be a papain-like novel cysteine peptidase.

The sequence alignment of MACP-II amino-terminus LPEQFEXPXQF also suggested that it is a papain-like enzyme. Table 1 shows the comparison of the biochemical properties of MACP-II with those of other dipteran and lepidopteran Cathepsin B-like peptidases. For comparative purposes, the

Fig. 3. Purification of 40–46-h APF cystein peptidases. **A:** Gel filtration elution profile. A 30–70% ammonium sulphate fraction was applied to a Sephacryl S-200 column. Open triangles = Protein concentration (A_{280}). Solid squares = Enzymatic activity monitored by cleavage of Z-FR-AMC substrate. **B,C:** Cation-exchange chromatography. Fractions I and II as in A were first chromatographed in covalent Thiol-Sepharose columns and the respective active peaks were poured in Mono-S columns and eluted as shown. Straight lines indicate NaCl linear gradients; (—) protein concentration; (•) enzyme activity. The insets to B and C show the respective SDS-PAGE of the unbound (lane 1) and eluted (lane 2) substances from Thiol-Sepharose columns. Vertical arrows indicate the selected active fractions coined MACP-I (B) and MACP-II (C).

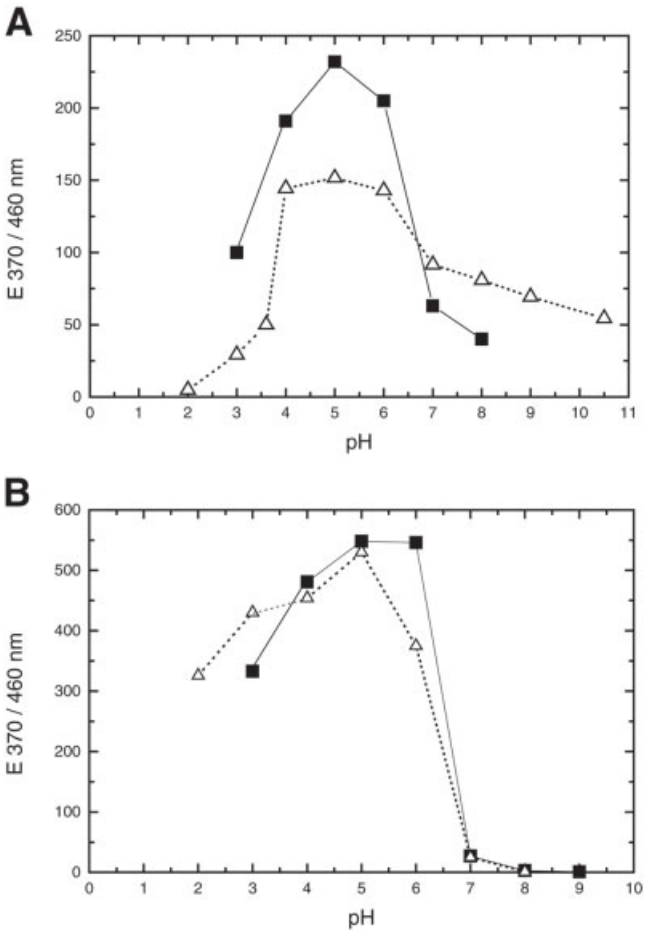

Fig. 5. Optimum pH and stability of the purified cystein proteases. The activity was measured using Z-FVR-AMC for MACP-I and Z-FR-AMC for MACP-II as subtrates. The pH stability was determined by pre-incubation of the enzymes in the absence of subtrates (120 min for MACP-I and 15 min for MACP-II). The residual enzymatic activity was then measured as described in Materials and Methods. Optimum pH (solid squares) and pH stability (open triangles) of MACP-I (**A**) and MACP-II (**B**).

human cathepsin B was included. The average molecular masses and pI values of other insect Cathepsin B's are calculated from their amino acid sequences (mature form) as described by Gasteiger et al. (2005). In general, the molecular mass of a large group of cysteine peptidases belonging to clan CA include papain, different cathepsins, insect homologs of papain, viral and parasite peptidases, ranging from 24 to 30 kDa (Rawlings and Barrett, 2004). The calculated MW of different insect cathepsins B range from 26,201 to 28,268 Da, which

TABLE 1. Calculated Molecular Mass (MW) and Isoelectric Point (p*I*) of Insect-Type Cathepsin B in Comparison With *C. capitata* MAPC-II and Human Cathepsin B. (D): Diptera; (L): Lepidoptera

Source		GenPept	Length[a] (aa)	MW (Da)	p*I*
C. capitata MACP-II	D	—	—	30,000[b]	5.85
A. gambiae	D	EAA09183[c]	239	26,201	6.55
D. melanogaster	D	AAF48317[d]	249	27,500	6.23
G. morsitans	D	AAK07477[e]	248	27,628	6.56
S. peregrina	D	BAA04103f	256	28,268	6.10
B. mori	L	BAB40804[g]	247	27,376	5.79
H. armigera	L	AAF35867[h]	247	27,490	6.06
L. obliqua	L	AAV91452[i]	247	27,019	5.78
H. sapiens	—	AAA52129[j]	248	27,119	5.21

[a]Length of the mature form.
[b]Experimental data from SDS-PAGE in Figure 4A.
[c]Holt et al., 2002.
[d]Adams et al., 2000.
[e]Yan et al., 2002.
[f]Takahashi et al., 1993.
[g]Xu and Kawasaki, 2001.
[h]Zhao et al., 2002.
[i]Veiga et al., 2005.
[j]Chan et al., 1986.

are of similar magnitude to that of the human homolog (Table 1). The higher apparent molecular mass (around 30 kDa, Fig. 4A, Table 1) of MACP-II might be due to glycosylation, which occurs in human cathepsin B at Asn^{192} and Asn^{289} (Chan et al., 1986). Three putative N-glycosylation sites were also reported for the *S. peregrina* homolog (calculated MW: 28,268 Da) (Takahashi et al., 1993). Insect cathepsin B's pI values range from pH 5.78 to 6.10, whereas MACP-II's pI was pH 5.85 (Table 1). Interestingly, cathepsin B's from Diptera have a pI ranging from pH 6.10 to 6.55, whereas those from Lepidoptera range from pH 5.78 to 6.06. Thus, MACP-II pI is closer to the lepidopteran group than to that of other flies. MACP-II as well as other insect cathepsin B's exhibit biochemical features that are shared by human cathepsin B such as substrate specificity, optimum pH, and pH stability (Turk et al., 1994). Moreover, the previously reported optimum pH of insect cathepsin B and that of MACP-II are similar, respectively, pH 5.0 and 6.0 (Shiba et al., 2001; Hernandez et al., 2003).

Kurata et al. (1992a) reported the isolation of a 29-kDa hemocyte cysteine peptidase involved in the dissociation of the flesh fly *S. peregrina* larval fat body. After pupariation, pupal hemocytes specifically express a 200-kDa surface protein essential for recognition of the fat body cell basement

membrane (Kobayashi et al., 1991). Then, the hemocyte cysteine peptidase is excreted, digesting the basement membrane and starting the fat body cell dissociation (Kurata et al., 1992b). Dorsey and Lockshin (1983) reported that a cathepsin B-like peptidase is active during the degradation of the abdominal intersegmental muscles of the moth, *Manduca sexta*. Cathepsin B was found in the phagosomes of *Drosophila* S2 cells (Kocks et al., 2003), the gut of the tsetse fly (Yan et al., 2002), the ovarian follicles of the mosquito, *Culex pipiens* (Uchida et al., 2001), and in the flesh fly *S. peregrina* (Homma, 2004). In particular, a cathepsin B related to vitellogenin digestion was described in the mosquito *Aedes aegypti* (Cho et al., 1999). Other papain-like enzymes were described in different hemimetabolous and holometabolous insects (Homma, 2004).

We can conclude that the novel cysteine peptidases of *C. capitata* described here seem to play an important role during early metamorphosis. Two of them, MACP-I and MACP-II, were purified to homogeneity and some of their biochemical properties were determined. The results of this study, together with previously published data (Rabossi et al., 2004, Gui et al., 2006), suggest that these peptidases might participate in tissue dissociation and degradation during pupation.

ACKNOWLEDGMENTS

The authors are grateful to Dr. Anka Ritonja for N-terminal sequencing and Dr. Karl Kramer (Manhattan, KS) for a critical reading of the manuscript. L.A.Q.A. and A.R. are career investigators of the CONICET. This work was supported by grants from the University of Buenos Aires, CONICET, and ANPCyT of Argentina to L.A.Q.A., and grant P1-0140 from the Ministry of Higher Education, Science and Technology of the Republic of Slovenia to V.T.

LITERATURE CITED

Adams MD, et al. (Drosophila Genome Consortium). 2000. The genome sequence of *Drosophila melanogaster*. Science 287:2185–2195.

Altschul SF, Gish W, Miller W, Myers EW, Lipman DJ. 1990. Basic local alignment search tool. J Mol Biol 215:403–410.

Boccaccio GL, Quesada-Allue LA. 1989. In vivo biosynthesis of a stage specific cuticle glycoprotein during early metamorphosis of the Medfly *Ceratitis capitata*. Biochem Biophys Res Comun 164:251–258.

Brocklehurst K, Carlsson J, Kierstan MP, Crook EM. 1973. Covalent chromatography. Preparation of fully active papain from dried papaya latex. Biochem J 133:573-584.

Brown DP, Wilkinson HS, Jongsma MA, Gatehouse JA. 2004. Characterisation of cysteine proteinases responsible for digestive proteolysis in guts of larval western corn rootworm *Diabrotica virgifera* by expression in the yeast *Pichia pastoris*. Insect Biochem Mol Biol 34:305–320.

Chan SJ, San Segundo B, McCormick MB, Steiner DF. 1986. Nucleotide and predicted amino acid sequences of cloned human and mouse preprocathepsin B cDNAs. Proc Natl Acad Sci USA 83:7721–7725.

Cho WL, Tsao SM, Hays AR, Walter R, Chen JS, Snigirevskaya ES, Raikhel AS. 1999. Mosquito cathepsin B-like protease involved in embryonic degradation of vitellin is produced as a latent extraovarian precursor. J Biol Chem 274:13311–13321.

Dorsey AM, Lockshin RA. 1983. Spontaneous degradation of insect myosin during metamorphic cell death conditions for proteolysis. Insect Biochem 13:11–18.

Gasteiger E, Hoogland C, Gattiker A, Duvaud S, Wilkins MR, Appel RD, Bairoch A. 2005. *Protein identification and analysis tools on the ExPASy Server.* In: Walker JM, editor. The proteomics protocols handbook. Totowa, NJ: Humana Press. p 571–607.

Gui ZZ, Lee KS, Kim BY, Choi YS, Wei YD, Choo YM, Kang PD, Yoon HJ, Kim I, Je YH, Seo SJ, Lee SM, Guo X, Sohn HD Jin BR. 2006. Functional role of aspartic proteinase cathepsin D in insect metamorphosis. BMC Dev Biol 6:49; doi: 10.1186/1471-213X-6-49.

Hernandez CA, Pujol M, Alfonso-Rubi J, Armas R, Coll Y, Perez M, Gonzalez A, Ruiz M, Castanera P, Ortego F. 2003. Proteolytic gut activities in the rice water weevil, *Lissorhoptrus brevirostris Suffrian* (Coleoptera: Curculionidae). Arch Insect Biochem Physiol 53:19–29.

Holt RA, et al. (Anopheles Genome Consortium). 2002. The

genome sequence of the malaria mosquito *Anopheles gambiae*. Science 298:129–149.

Homma KJ. 2004. Insect homologs of papain. In: Barrett AJ, Rawlings ND, Woessner JF, editors. Handbook of proteolytic enzymes, vol. II. Amsterdam: Elsevier. p 1189–1192.

Kawamura M, Wadano A, Miura K. 1984. Purification and some properties of cathepsin-like thiol protease from pupae of the blowfly *Aldrichina grahami*. Comp Biochem Physiol B 78:279–286.

Kobayashi H, Kurata S, Natori S. 1991. Purification of the 200 KDa membrane protein of *Sarcophaga peregrina* and its specific interaction with fat body. Insect Biochem 21:517–522.

Kocks C, Maehr R, Overkleeft HS, Wang EW, Iyer LK, Lennon-Dumenil AM, Ploegh HL, Kessler BM. 2003. Functional proteomics of the active cysteine protease content in *Drosophila* S2 cells. Mol Cell Proteomics 2:1188–1197.

Kurata S, Saito H., Natori S. 1990. Participation of hemocyte proteinase in dissociation of the fat body on pupation of *Sarcophaga peregrina* (Flesh fly). Insect Biochem 20:461–465.

Kurata S, Saito H, Natori S. 1992a. Purification of a 29-kDa hemocyte proteinase of *Sarcophaga peregrina*. Eur J Biochem 204:911–914.

Kurata S, Saito H, Natori, S. 1992b. The 29-KDa hemocyte proteinase dissociates fat body at metamorphosis of *Sarcophaga*. Dev Biol 153:115–121.

Quesada-Allué LA, Rabossi A, Wappner P. 1994. Growth in the laboratory. In: Quesada-Allué LA, editor. The Mediterranean fruit fly. Laboratory manual. Buenos Aires: YPF Press. p 24–31.

Rabossi A, Boccaccio GL, Wappner P, Quesada-Allué LA. 1991. Morphogenesis and cuticular markers during the larval-pupal transformation of the Medfly *Ceratitis capitata*. Entomol Exp Applicata 60:135–141.

Rabossi A, Wappner P, Quesada-Allué LA. 1992. Larva to pharate adult transformation in the Medfly, *Ceratitis capitata*. Can Entomol 1241139–1147.

Rabossi A, Quesada-Allué LA. 2000. Metamorphosis-associated proteolysis in *Ceratitis capitata*. Entomol Exp Applicata 94:57–65.

Rabossi A, Stoka V, Puizdar V, Turk V, Quesada-Allué LA. 2004. Novel aspartyl proteinase associated to fat body histolysis during *Ceratitis capitata* early metamorphosis. Arch Insect Biochem Physiol 57:51–67.

Rawlings ND, Barrett AJ. 2004. Introduction: the clans and families of cysteine peptidases. In: Barrett AJ, Rawlings ND, Woessner JF, editors. Handbook of proteolytic enzymes, vol. II. Amsterdam: Elsevier. p 1051–1071.

Riddiford LM, Hiruma K, Zhou X, Nelson CA. 2003. Insights into the molecular basis of the hormonal control of molting and metamorphosis from *Manduca sexta* and *Drosophila melanogaster*. Insect Biochem Mol Biol 33:1327–1338.

Scott RC, Schuldiner O, Neufeld TP. 2004. Role and regulation of starvation-induced autophagy in the Drosophila fat body. Dev Cell 7:167–178.

Shiba H, Uchida D, Kobayashi H, Natori M. 2001. Involvement of cathepsin B- and L-like proteinases in silk gland histolysis during metamorphosis of *Bombyx mori*. Arch Biochem Biophys 390:28–34.

Takahashi N, Kurata S, Natori S. 1993. Molecular cloning of cDNA for the 29 kDa proteinase participating in decomposition of the larval fat body during metamorphosis of *Sarcophaga peregrina* (flesh fly). FEBS Lett 334:153–157.

Turk B, Dolenc I, Zerovnik E, Turk D, Gubensek F, Turk V. 1994. Human cathepsin B is a metastable enzyme stabilized by specific ionic interactions associated with the active site. Biochemistry 33:14800–14806.

Uchida K, Ohmori D, Ueno T, Nishizuka M, Eshita Y, Fukunaga A, Kominami E. 2001. Preoviposition activation of cathepsin-like proteinases in degenerating ovarian follicles of the mosquito *Culex pipiens pallens*. Dev Biol 237:68–78.

Veiga ABG, Ribeiro JMC, Guimaraes JA, Francischetti IMB. 2005. A catalog of *Lonomia obliqua* transcripts and proteins probably involved in the hemorrhagic syndrome. Gene 355:11–27.

Xu Y, Kawasaki H. 2001. Isolation and expression of cathepsin B cDNA in hemocytes during metamorphosis of *Bombyx mori*. Comp Biochem Physiol B 130:393–399.

Yan J, Cheng Q, Li CB, Aksoy S. 2002. Molecular characterization of three gut genes from *Glossina morsitans morsitans*: cathepsin B, zinc-metalloprotease and zinc-carboxypeptidase. Insect Mol Biol 11:57–65.

Yang XM, Hou LJ, Dong DJ, Shao HL, Wang JX, Zhao XF. 2006. Cathepsin B-like proteinase is involved in the decomposition of the adult fat body of *Helicoverpa armigera*. Arch Insect Biochem Physiol 62:1–10.

Zdarek J. 1985. Regulation of pupariation in flies. In: Kerkut GA, Gilbert LI, editors. Comparative insect physiology, biochemistry and pharmacology, vol. 10. New York: Pergamon Press. p 301–333.

Zdarek J, Friedman S. 1986. Pupal ecdysis in flies: mechanisms of evagination of the head and expansion of the thoracic appendages. J Insect Physiol 32:917–923.

Zhao XF, Wang JX, Xu XL, Schmid R, Wieczorek H. 2002. Molecular cloning and characterization of the cathepsin B-like proteinase from the cotton boll worm, *Helicoverpa armigera*. Insect Mol Biol 11:567–575.

Zhao XF, Wang JX, Li FX, Sueda S, Kondo H. 2005. Analysis of substrate specificity and endopeptidyl activities of the cathepsin B-like proteinase from *Helicoverpa armigera*. Protein J 24:219–225.